

SCTN: Sparse Convolution-Transformer Network for Scene Flow Estimation

Bing Li Cheng Zheng Silvio Giancola Bernard Ghanem
Visual Computing Center, KAUST, Thuwal, Saudi Arabia

Abstract

We propose a novel scene flow estimation approach to capture and infer 3D motions from point clouds. Estimating 3D motions for point clouds is challenging, since a point cloud is unordered and its density is significantly non-uniform. Such unstructured data poses difficulties in matching corresponding points between point clouds, leading to inaccurate flow estimation. We propose a novel architecture named Sparse Convolution-Transformer Network (SCTN) that equips the sparse convolution with the transformer. Specifically, by leveraging the sparse convolution, SCTN transfers irregular point cloud into locally consistent flow features for estimating continuous and consistent motions within an object/local object part. We further propose to explicitly learn point relations using a point transformer module, different from existing methods. We show that the learned relation-based contextual information is rich and helpful for matching corresponding points, benefiting scene flow estimation. In addition, a novel loss function is proposed to adaptively encourage flow consistency according to feature similarity. Extensive experiments demonstrate that our proposed approach achieves a new state of the art in scene flow estimation. Our approach achieves an error of 0.038 and 0.037 (EPE3D) on FlyingThings3D and KITTI Scene Flow respectively, which significantly outperforms previous methods by large margins.

1. Introduction

Understanding 3D dynamic scenes is critical to many real-world applications such as autonomous driving and robotics. Scene flow is the 3D motion of points in a dynamic scene, which provides low-level information for scene understanding [55, 29, 13]. The estimation of the scene flow can be a building block for more complex applications and tasks such as 3D object detection [67, 46], segmentation [52, 23] and tracking [66, 42]. With the increasing popularity of point cloud data, it is desirable to estimate 3D motions directly from 3D point clouds. However, many previous scene flow methods estimate the 3D motion from stereo or RGB-D images. Only a few works *e.g.* [62, 29, 39]

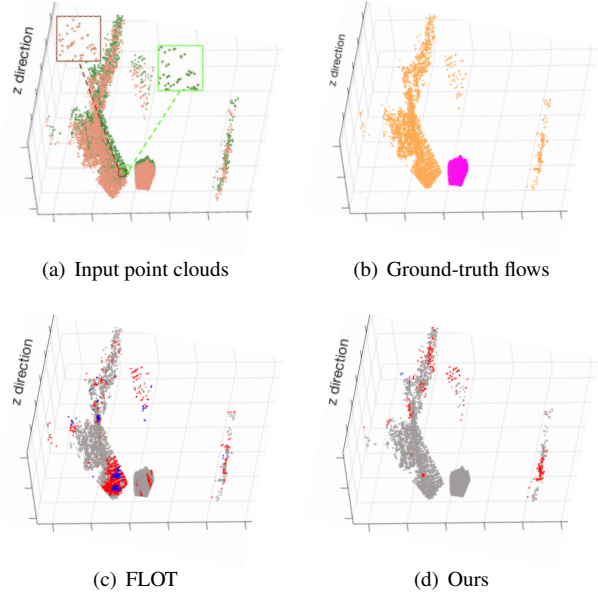


Figure 1: **Qualitative results of SCTN.** (a) Brown and green indicate the first and second point clouds, where the brown and green blocks zoom in a pair of corresponding regions between point clouds. However, these regions are visually dissimilar, posing difficulties in scene flow estimation. (b) Ground-truth scene flow, where similar colors indicate consistent flows. (c-d) Gray, red and blue color indicate small, medium and large errors of flow estimation in (c) and (d). Our SCTN better estimates flows than FLOT.

tackle scene flow from point clouds.

Recent methods [62, 29, 14] such as FLOT [39] propose deep neural networks to learn scene flow from point clouds in an end-to-end way, which achieves promising estimation performance. However, estimating scene flow from point clouds is still challenging in two aspects. First, due to the significantly non-uniform density and unordered nature of 3D point clouds, it is difficult to match corresponding points between point clouds, leading to inaccurate flow estimation. Specifically, as shown in Figure 1(a), two local regions marked by the brown block and green one correspond to each other between point clouds, however, are visually

different. Nevertheless, existing methods [29, 39] extract the feature for each point by aggregating information only from its local neighborhood. Such feature representation is not rich enough to measure the correlations of corresponding points in these two local regions of Figure 1(a). Consequently, these methods often infer inaccurate 3D scene flows (e.g. Figure 1 (c)) in regions with complex structure or various density.

The second challenge lies in that the points usually undergo coherent and consistent motions in local regions of a rigid or non-rigid object (e.g. pedestrians and cyclists). Yet, this concept is mostly ignored by recent work in scene flow [29, 39, 62]. Ideally, we would like to enforce the predicted flows in a local region of an object to be *consistent* and *smooth* in 3D space. An ideal solution would be to leverage instance segmentation labels and learn object-wise motions. However, such labels are not necessarily available for point cloud in scene flow datasets. Instead of relying on instance-level segmentation label, we argue that such flows can be approximately achieved by enforcing a feature consistency among points in a local region.

In this work, we resort in feature representations and loss functions to estimate accurate scene flow from point clouds. In particular, we explore novel feature representations (information) that would help to infer an accurate and locally consistent scene flows. We therefore propose a Sparse Convolution-Transformer Network (SCTN) which incorporates a Sparse Convolution module from voxelized point cloud with a Transformer module at the point level for scene flow estimation. The sparse convolution module transfers irregular point cloud into locally consistent flow features for estimating coherent motions within an object /local object parts. On the other hand, sparse convolution suffers the issue of information loss for achieving large receptive fields, as revealed in [49]. To complement the sparse convolution module, we propose to additionally learn point relations in the feature space to capture important contextual information. Inspired by impressive performance of transformer in object detection tasks [3], we propose a transformer module to explicitly learn point relation for capturing complementary information.

In addition, we propose a new loss function for training, which adaptively controls the flow consistency according to the similarity of point features. Our experiments demonstrate that this novel SCTN architecture significantly outperforms state-of-the-art method on standard scene flow datasets: FlyingThings3D [36] and KITTI Scene Flow [34].

Contributions. Our contributions are fourfold:

1. We propose a novel end-to-end network named SCTN that incorporates the advantages of the sparse convolution and transformer.
2. We propose a new consistency loss, improving the generalization capability of the trained scene flow model.
3. We are the first to introduce transformer for scene flow estimation. Our method shows that the transformer module provides complementary information and improves the accuracy of the scene flow estimation via modeling point relationship.
4. Our method outperforms the state-of-the-art methods with remarkable margins on both FlyingThings3D [36] and KITTI Scene Flow [34] benchmarks.

2. Related Work

Optical Flow. Optical flow estimation is defined as the task of predicting the pixels motions between consecutive 2D video frames. Optical flow is a fundamental tool for 2D scene understanding, that have been extensively studied in the literature. Traditional methods [17, 1, 65, 60, 2, 44] address the problem of estimating optical flow as an energy minimization problem, that does not require any training data. Dosovitskiy *et al.* [11] proposed a first attempt for an end-to-end model to solve optical flow based on convolution neural network (CNN). Inspired by this work, many CNN-based studies have explored data-driven approaches for optical flow [11, 33, 21, 20, 19, 48, 51].

Scene Flow from Stereo and RGB-D Videos. Estimating scene flow from stereo videos have been studied for years [6, 56, 59, 22, 24, 50]. Many works estimate scene flow by jointly estimating stereo matching and optical flow from consecutive stereo frames [37]. Similar to optical flow, traditional methods formulate scene flow estimation as an energy minimization problem [18, 59]. Recent works estimate scene flow from stereo video using neural networks [6]. For example, networks for disparity estimation and optical flow are combined in [22, 32]. Similarly, other works [43, 47] explore scene flow estimation from RGB-D video.

Scene Flow on Point Clouds. Inspired by FlowNet [11], FlowNet3D [29] propose an end-to-end network to estimate 3D scene flow from raw point clouds. Different from traditional methods [10, 54], FlowNet3D [29] is based on PointNet++ [41], and propose a flow embedding layer to aggregate the information from consecutive point clouds and extract scene flow with convolutional layers. FlowNet3D++ [58] improves the accuracy of FlowNet3D by incorporating geometric constraints. HPLFlowNet [15] projects point clouds into permutohedral lattices, and then estimates scene flow using Bilateral Convolutional Layers. Inspired by the successful optical flow method PWC-Net [48], PointPWC [62] estimates scene flow in a coarse-to-fine fashion, introducing cost volume, upsampling, and warping modules for the point cloud processing. The most related recent work to our approach is FLOT [39]. FLOT addresses the scene flow as a matching problem between corresponding points in the consecutive clouds and solve it using optimal transport. Our method differs from FLOT [39] in two aspects. First, our method ex-

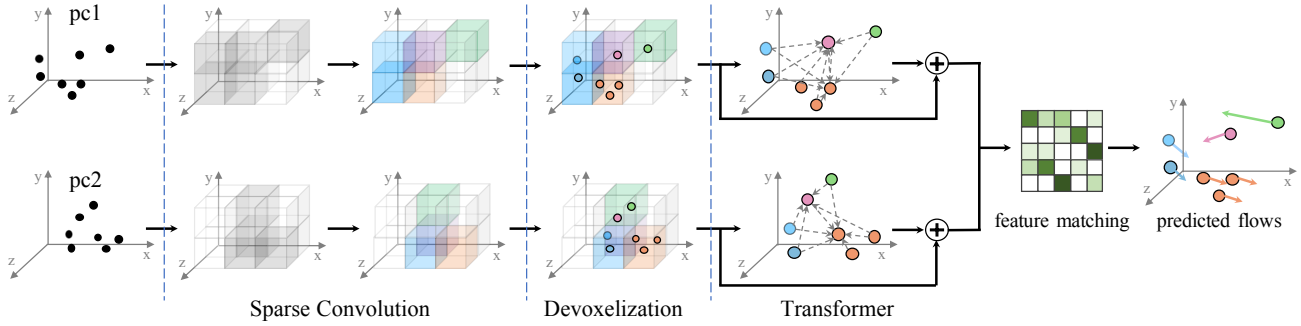


Figure 2: **Overall framework of our SCTN approach.** Our SCTN voxelizes the input point clouds and extracts features for voxels by the sparse convolution module. The voxel features are then projected back into point features via devoxelization. These point features are fed into the transformer module to explicitly learn point relations. With the point features from our sparse convolution and transformer module, SCTN conducts feature matching between the point clouds and predicts flows.

Explicitly explores more suitable feature representation that facilitate the scene flow estimation. Second, our method is trained to enforce the consistency of predicted flows for local-region points from the same object, which is ignored in FLOT [39]. Recently, Gojcic *et al.* [14] explore weakly supervised learning for scene flow estimation using labels of ego motions as well as ground-truth foreground and background masks. Other works [62, 26, 35] study unsupervised/self-supervised learning for scene flow estimation on point clouds, proposing regularization losses that enforces local spatial smoothness of predicted flows. These losses are directly constraining points in a local region to have similar flows, but are not feature-aware.

3D Deep Learning. Recently, many works introduced deep representation for point cloud classification and segmentation [41, 52, 68, 30, 61, 28, 27]. Qi *et al.* [40] propose PointNet that learns point feature only from point positions. PointNet++ [41] extends PointNet by aggregating information from local regions. Motivated by PointNet++, many works [68, 52, 27, 28] design various local aggregation functions for point cloud classification and segmentation. Different from these point-based convolutions, [63, 57] transform point cloud into voxels, such that typical 3D convolution can be applied. However, such voxel-based convolution suffer from expensive computational and memory cost as well as information loss during voxelization. Liu *et al.* [31] combine pointnet [40] with voxel-based convolution to reduce the memory consumption. For the sake of efficient learning, researchers have explored sparse convolution for point cloud segmentation [64, 8] which shows impressive performance. Tang *et al.* [49] propose to combine pointnet with sparse convolution for large-scale point cloud segmentation. Differently, we not only leverage feature representation by the efficient sparse convolution module for scene flow estimation, but also introducing a transformer module to provide complementary information.

3. Methodology

Figure 2 illustrates the overall framework of our approach, that takes two consecutive point clouds \mathcal{P} and \mathcal{Q} as inputs and predict the scene flow from \mathcal{P} to \mathcal{Q} . First, we convert both point clouds into voxels, from which we apply several layers of sparse convolution (3.1). Then, the voxel features are projected back into the original 3D points. Second, our transformer module improves the point representation by modeling relation between points. (3.2). Third, with features extracted by sparse convolution and transformer module, we calculate a feature matching matrix between \mathcal{P} and \mathcal{Q} , where a sinkhorn algorithm [39, 9, 7] is leveraged to predict the flows (3.3). We train our method with an extra regularizing loss that enforces spatial consistency between the features in neighboring regions (3.4).

Formally, we define $\mathcal{P} = \{p_i\}_{i=1}^{n_{\mathcal{P}}}$ and $\mathcal{Q} = \{q_j\}_{j=1}^{n_{\mathcal{Q}}}$ two point clouds with p_i and q_j the 3D coordinates of i -th and j -th point in \mathcal{P} and \mathcal{Q} , respectively. We cast the problem of scene flow estimation as a point correspondences prediction from the points in \mathcal{P} to the points in \mathcal{Q} . In particular, we denote \tilde{p}_i the predicted corresponding position of p_i in \mathcal{Q} and define the predicted scene flow \mathbf{u}_i of p_i as $\mathbf{u}_i = \tilde{p}_i - p_i$. In the following, we will describe the feature representation of point in \mathcal{P} for clarity. Points in \mathcal{Q} employ the same feature extraction as \mathcal{P} .

3.1. Sparse Convolution based Point Representation

We proposed two kinds of point features, from the sparse convolution and the transformer modules such that our method can match proper correspondences to predict accurate scene flows. This subsection describes our sparse convolution module first.

We aim to extract consistent features for points in a local region from the same object for estimating locally smooth and consistent motions. To this end, we rely on a sparse convolution backbone on voxelized point clouds, different

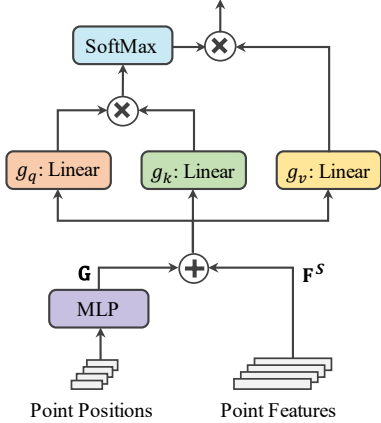


Figure 3: **Details of our Transformer module.** \otimes and \oplus correspond to matrix multiplication and addition operations, respectively.

from existing methods [39, 29, 62] that rely on point-based convolutions (e.g. PointNet++ [41]), We argue that such voxel-based convolution ensure points in a local neighborhood to have smoother features, ideally leading to consistent flows in space.

Voxel features via sparse convolution. Formally, given the point cloud \mathcal{P} (similarly \mathcal{Q}), we first discretize the points into voxels, then leverage a U-Net [45] architecture network built with Minkowski Engine [8] to compute the non-empty voxel’s feature. More details are available in our supplementary material.

Point feature via Devoxelization. We project back the voxel features into point feature \mathbf{F}_i^S for point p_i . In particular, we interpolate the point features from the k closest voxels following equation (1). $\mathcal{N}^v(p_i)$ represents the set of K nearest neighboring non-empty voxels for the point p_i , $\mathbf{v}_k \in \mathbb{R}^C$ represents the feature of k -th closest non-empty voxels and d_{ik} the Euclidian distance between the point p_i and the center of the k -th closest non-empty voxel.

$$\mathbf{F}_i^S = \frac{\sum_{k \in \mathcal{N}^v(p_i)} d_{ik}^{-1} \cdot \mathbf{v}_k}{\sum_{k \in \mathcal{N}^v(p_i)} d_{ik}^{-1}} \quad (1)$$

We observed that our sparse convolution module encourages close points to have similar features, which helps our method generate consistent flows for these points. This is favorable for local object parts or rigid objects with dense densities and consistent flows (e.g. LiDAR points on a car at close range).

3.2. Transformer based Point Representation

Our sparse convolution module has to adopt aggressive downsampling to obtain a large receptive field, as suggested by [49]. However, aggressive downsampling inevitably loses some important information [49]. In such case, the

features of points with large information loss are disadvantageous for estimating their scene flow. For example, given neighboring points that belong to two objects with different motions, their features may be indiscriminable, leading to inaccurate flow estimations. To address this issue, we explicitly exploit point relations as a complementary information on top of the point feature extracted with sparse convolution. Recent work [71, 69, 3] employ transformer and self-attention to model internal relation in the features, achieving impressive performance in image tasks such as detection and recognition. Similar trend appeared in point cloud classification and segmentation [16, 70, 12] showing the effectiveness of transformer in 3D. Inspired by these work, we resort to transformer for capturing point relation information as the point feature.

In an autonomous navigation scenario, point clouds represent complete scenes, with small object such as cars and trucks, but also large structure such as buildings and walls. The scene flows in such a large scene do not only depend on the aggregation from a small region, but rather a large one. As a results, we refrain in building a transformer for the local neighborhood as it would restrict the receptive field or require deeper model (i.e. increase the memory). Instead, our transformer module learns the relation of each point to all other points, such that the transformer can adaptively capture the rich contextual information contained in the complete scene.

Formally, given a point p_i , we consider every points in \mathcal{P} as query and key elements. Our transformer module builds a point feature representation for p_i by adaptively aggregating the features of all points based on self-attention:

$$\mathbf{F}_i^R = \sum_{j=1}^{n_p} A_{i,j} \cdot g_v(\mathbf{F}_j^S, \mathbf{G}_j) \quad (2)$$

where g_v is the a learnable function (e.g. linear function), $A_{i,j}$ is an attention defining a weight of p_j to p_i , \mathbf{G}_j is the positional encoding feature of p_j .

As pointed in literature [69, 3], the positional encoding feature can provide important information for the transformer. The position encoding in recent transformer work [70] encodes the *relative* point position to neighbors for point cloud classification or segmentation. Different from those tasks, the task of scene flow is to find correspondences between consecutive point clouds. Thus, we argue that an *absolute* position provides sufficient information to estimate the scene flow. Therefore, given a point p , our position encoding function encodes its *absolute* position p_j :

$$\mathbf{G}_j = \phi(p_j) \quad (3)$$

where ϕ is a MLP layer. Using absolute positions also reduced computational cost, compared with using relative positions.

We calculate an attention $A_{i,j}$ defined by the similarity between the features of p_i and p_j in an embedding space. The similarity is estimated using features and position information:

$$A_{i,j} \propto \exp\left(\frac{(g_q(\mathbf{F}_i^S, \mathbf{G}_i))^T \cdot g_k(\mathbf{F}_j^S, \mathbf{G}_j)}{c_a}\right) \quad (4)$$

where $g_q(\cdot, \cdot)$ and $g_k(\cdot, \cdot)$ are the learnable mapping functions to project feature into an embedding space, and c_a is the output dimension of $g_q(\cdot, \cdot)$ or $g_k(\cdot, \cdot)$. $A_{i,j}$ is further normalized such that $\sum_j A_{i,j} = 1$. The architecture of our transformer module is illustrated in Figure 3.

3.3. Flow Prediction

We cast the flow prediction as a feature correspondences matching problem, following [39]. Since the point feature from our transformer module and our sparse convolution module provide complementary information, we fuse the two kinds of features through skip connection for p_i *i.e.* $\mathbf{F}_i = \mathbf{F}_i^S + \mathbf{F}_i^R$

Based on the point features from \mathcal{P} and \mathcal{Q} , we compute a matrix of feature correlation $\mathbf{C} \in \mathbb{R}^{n_{\mathcal{P}} \times n_{\mathcal{Q}}}$ between the points in \mathcal{P} and \mathcal{Q} . Formally, with $\mathbf{F}_i^{\mathcal{P}}$ and $\mathbf{F}_j^{\mathcal{Q}}$ being the features from two points in \mathcal{P} and \mathcal{Q} , the correlation $\mathbf{C}_{i,j}$ between $p_i \in \mathcal{P}$ and $p_j \in \mathcal{Q}$ is computed as follows:

$$\mathbf{C}_{i,j} = 1 - \frac{(\mathbf{F}_i^{\mathcal{P}})^T \cdot \mathbf{F}_j^{\mathcal{Q}}}{\|\mathbf{F}_i^{\mathcal{P}}\|_2 \|\mathbf{F}_j^{\mathcal{Q}}\|_2} \quad (5)$$

We then adopt the Sinkhorn algorithm that estimate soft correspondences from the correlation matrix \mathbf{C} and predict flows for \mathcal{P} , following FLOT [39]. We further refine the estimated flows with a few convolutional layers similar to FLOT [39].

3.4. Training Losses

We train our model to regress the scene flow in a supervised fashion, on top of which we propose a Feature-aware Spatial Consistency loss, named ‘‘FSC loss’’, that enforces similar features to have similar flow. The FSC loss provides a better generalization and transfer capability between the training and testing datasets.

Supervised loss. We define in Equation (6) our supervised loss E^s that minimize the L_1 -norm difference between the estimated flow and the ground truth flow for the non-occluded points. \mathbf{u}_i^* and \mathbf{u}_i are respectively the ground-truth and predicted motion flow for the point $p_i \in \mathcal{P}$ and m_i is a binary indicator for the non-occlusion of this point, *i.e.* $m_i = 0$ if p_i is occluded, otherwise $m_i = 1$.

$$E^s = \sum_i^N m_i \|\mathbf{u}_i - \mathbf{u}_i^*\| \quad (6)$$

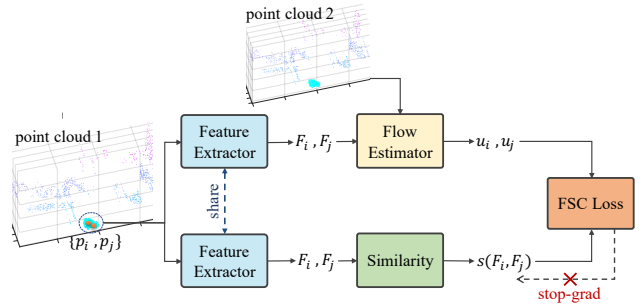


Figure 4: **Stop gradient for the FSC loss.** We extract the flow from a neighboring point as well as the similarity between their features. We optimize the FSC loss without back-propagating the gradients to the features from the similarity branch to avoid degenerate cases.

Feature-aware Spatial Consistency (FSC) loss. Given a local region, points from the same object usually has consistent motions, resulting in similar flows. To model such phenomena, we propose a consistency loss that ensures points within an object/local object part to have similar predicted flows. Yet, object annotations are not necessarily available. Instead, we propose to control flow consistency according to feature similarity. That is, given a local region, if two points are of larger feature similarity, they are of the higher probability that belongs to the same object.

In particular, given a point p_i with predicted flow \mathbf{u}_i and its local neighborhood $\mathcal{N}(p_i)$, we enforce the flow \mathbf{u}_j of $p_j \in \mathcal{N}(p_i)$ to be similar to \mathbf{u}_i , if the feature \mathbf{F}_i of p_j is similar to \mathbf{F}_j of p_j . Formally, we define the FSC loss as follows:

$$E^c = \sum_{i=1}^N \sum_{p_j \in \mathcal{N}(p_i)} s(\mathbf{F}_i, \mathbf{F}_j) \cdot \|\mathbf{u}_i - \mathbf{u}_j\|_1 \cdot \Gamma \quad (7)$$

where the similarity function $s(\mathbf{F}_i, \mathbf{F}_j)$ of p_i and p_j is defined as $1 - \exp(-(\mathbf{F}_i)^T \cdot \mathbf{F}_j / \tau)$ with τ being a temperature hyper-parameter. We set $\Gamma = \varepsilon / (\|\mathbf{u}_i^*\|_1 + \varepsilon)$ to adaptively adjust flow differences according to p_i 's groundtruth flow \mathbf{u}_i^* , where ε is a hyper-parameter. Applying Γ with small ε allows points on fast-moving objects to have larger predicted flow differences than that on slow-moving objects.

A naive implementation of the FSC loss would inevitably lead to degenerate cases. In particular, the FSC loss is a product of two objectives: (i) a similarity $s(\mathbf{F}_i, \mathbf{F}_j)$ between the features \mathbf{F}_i and \mathbf{F}_j and (ii) a difference $\|\mathbf{u}_i - \mathbf{u}_j\|_1$ between their flows. The scope of this loss is to train the flows to be similar if they have similar features. However, to minimize the FSC loss, the model would make the point features \mathbf{F}_j and \mathbf{F}_i be orthogonal (*i.e.*, $\mathbf{F}_j \cdot \mathbf{F}_i = 0$), such that $s(\mathbf{F}_j, \mathbf{F}_i) = 0$ (*i.e.*, $E^c = 0$). Obviously, it is against our aim.

To circumvent this limitation, we propose a stop-gradient

for the point features fed into the FSC loss, taking inspiration from recent advances in self-supervised learning [5]. As illustrated in Figure 4, our architecture stops the propagation of the gradient in the branch extracting the feature similarity. By such architecture, our FSC loss avoids optimizing the features, while optimizing solely the flows similarities $\|\mathbf{u}_j - \mathbf{u}_i\|_n$ for neighboring points with similar features.

4. Experiments

Dataset. We conduct our experiments on two datasets that are widely used to evaluate scene flow. *FlyingThings3D* [36] is a large-scale synthetic stereo video datasets, where synthetic objects are selected from ShapeNet [4] and randomly assigned various motions. We generate 3D point clouds and ground truth scene flows with their associated camera parameters and disparities. Following the same preprocessing as in [39, 15, 62], we randomly sample 8192 points and remove points with camera depth greater than 35 m. We use the same 19640/3824 pairs of point cloud (training/testing) used in the related works [39, 15, 62]. *KITTI Scene Flow* [34, 8] is a real-world Lidar scan dataset for scene flow estimation from the KITTI autonomous navigation suite. Following the preprocessing of [15], we leverage 142 point cloud pairs of 8192 points for testing only. For a fair comparison, we also remove ground points by discarding points whose height is lower than -1.4m , following the setting of existing methods [39, 62, 15].

Evaluation Metrics. To evaluate the performance of our approach, we adopt the standard evaluation metrics used in the related methods [39, 62, 15], described as follows: The *EPE3D* (m) (3D end-point-error) is calculated by computing the average L_2 distance between the predicted and GT scene flow, in meters. This is our main metric. The *Acc3DS* is a strict version of the accuracy which estimated as the ratio of points whose $\text{EPE3D} < 0.05\text{m}$ or relative error $< 5\%$. The *Acc3DR* is a relaxed accuracy which is calculated as the ratio of points whose $\text{EPE3D} < 0.10\text{m}$ or relative error $< 10\%$. The *Outliers* is the ratio of points whose $\text{EPE3D} > 0.30\text{m}$ or relative error $> 10\%$.

Implementation Details. We implement our method in PyTorch [38]. We train our method on FlyingThing3D then evaluate on FlyingThing3D and KITTI. We minimize a cumulative loss $E = E^s + \lambda E^c$ with $\lambda = 0.35$ a weight that scale the losses. We use the Adam optimizer [25] with an initial learning rate of 10^{-3} , which is dropped to 10^{-4} after the 50^{th} epoch. First, we train for 40 epochs using only with the supervised loss. Then we continue the training for 20 epochs with both the supervision loss and the FSC loss, for a total on 60 epochs. The whole training takes about 30 hours. We use a voxel size of resolution 0.08m . For the FSC loss, we set $\tau = 0.39$ and $\varepsilon = 19$. Please refer to the supplementary material for further details.

4.1. Quantitative Evaluation

We compare our approach with recent deep-learning-based methods including FlowNet3D [29], HPLFlowNet [15], PointPWC [62] and FLOT [39]. These methods are state-of-the-art in scene flow estimation from point cloud data and do not leverage any additional labels such as ground-truth ego motions or instance segmentation.

Results on FlyingThings3D. We train and evaluate our model on the FlyingThings3D datasets. As shown in Table 1, our method outperforms all methods in every metrics by a significant margin. It is worth noting that our method obtains an EPE3D metric below 4cm , with a relative improvement of 26.9% and 35.5% over the most recent methods FLOT [39] and PointPWC [62], respectively. The performance shows that our method is effective in predicting flows with high accuracy.

Results on KITTI without Fine-tune. Following the common practice [39, 62], we train our model on FlyingThings3D and directly test the trained model on KITTI Scene Flow dataset, without any fine-tuning, to evaluate the generalization capability of our method. We report in Table 1 the highest accuracy of scene flow estimation on KITTI Scene Flow dataset for our SCTN method. Again, we reduce the EPE3D metric below 4cm , with a 33.9% relative improvement over FLOT [39]. In the Acc3DS metrics, our method outperforms both FLOT [39] and PointPWC [62] by 13.5% and 16.6% respectively. This results highlight the capability of our method to generalize well on real LiDAR scan dataset.

4.2. Qualitative Evaluation

To qualitatively evaluate the quality of our scene flow predictions, we visualize the errors in scene flow prediction in Figure 1 and 5. In particular, we quantize the flow estimation errors into *small*, *medium* and *large* errors. The small errors correspond to $\text{EPE3D} < 0.05\text{m}$, medium errors to $\text{EPE3D} \geq 0.05\text{m}$ and $\text{EPE3D} < 0.3\text{m}$, and large errors indicate $\text{EPE3D} \geq 0.3\text{m}$. We visualize the qualitative performances of FLOT [39] in comparison with SCTN. Figure 1 and 5 show that points from the same object usually have similar ground-truth flows. Yet, FLOT introduces medium errors in the car, highlighting the inconsistency in the scene flow predictions. FLOT also introduces medium and large errors in some regions for the background objects, even though those points have similar flows. In contrast, our method is more consistent in the prediction for points in the same object, achieving better performance, *e.g.* for the close car with higher density of points.

4.3. Ablation Study

We introduce three main components in our architecture, a sparse convolution backbone, a transformer module, and an FSC loss. To study their role, we ablate each proposed

Table 1: **Comparison with the state-of-the-art** on FlyingThings3D and KITTI. Best results in bold. Our proposed model SCTN reaches highest performances in all metrics.

Dataset	Method	EPE3D(m) ↓	Acc3DS ↑	Acc3DR ↑	Outliers ↓
FlyingThings3D	FlowNet3D [29]	0.114	0.412	0.771	0.602
	HPLFlowNet [15]	0.080	0.614	0.855	0.429
	PointPWC [62]	0.059	0.738	0.928	0.342
	EgoFlow [53]	0.069	0.670	0.879	0.404
	FLOT [39]	0.052	0.732	0.927	0.357
	SCTN (ours)	0.038	0.847	0.968	0.268
KITTI	FlowNet3D [29]	0.177	0.374	0.668	0.527
	HPLFlowNet [15]	0.117	0.478	0.778	0.410
	PointPWC [62]	0.069	0.728	0.888	0.265
	EgoFlow [53]	0.103	0.488	0.822	0.394
	FLOT [39]	0.056	0.755	0.908	0.242
	SCTN (ours)	0.037	0.873	0.959	0.179

Table 2: **Ablation for SCTN.** We further analyse the performances of our three components: the sparse convolution backbone, the transformer and the feature-aware spatial consistency loss. We highlight in bold the best performances.

Dataset	Transformer	FSC loss	EPE3D(m) ↓	Acc3DS ↑	Acc3DR ↑	Outliers ↓
FlyingThings3D			0.041	0.818	0.960	0.292
		✓	0.040	0.829	0.963	0.284
	✓		0.038	0.842	0.967	0.274
	✓	✓	0.038	0.847	0.968	0.268
KITTI			0.045	0.835	0.939	0.200
		✓	0.042	0.853	0.943	0.188
	✓		0.040	0.863	0.953	0.186
	✓	✓	0.037	0.873	0.959	0.179

Table 3: **Ablation of our contribution on FLOT.** We transfer our Transformer module and FSC loss to FLOT.

Dataset	Method	EPE3D(m) ↓	Acc3DS ↑	Acc3DR ↑	Outliers ↓
FlyingThings3D	FLOT	0.052	0.732	0.927	0.357
	FLOT + FSC loss	0.051	0.736	0.927	0.355
	FLOT + Transformer	0.044	0.792	0.952	0.309
	FLOT + Transformer + FSC loss	0.044	0.794	0.951	0.303
KITTI	FLOT	0.056	0.755	0.908	0.242
	FLOT + FSC loss	0.050	0.793	0.920	0.223
	FLOT + Transformer	0.043	0.835	0.941	0.197
	FLOT + Transformer + FSC loss	0.041	0.845	0.945	0.193

component of our model and evaluate their performance on both datasets. For all the experiments, we follow the same training procedure than in the main results. Table 2 reports the evaluation results.

Sparse convolution. Table 2 shows that our approach with the sole sparse convolution module already outperforms the state-of-the-art methods listed in Table 1. Different from the methods using point-based convolution, our method inter-

polates point feature from that of neighboring voxels, which ensures that points in a local region have consistent features, to some extent. The results show that such consistent point features are favorable for scene flow estimation.

Transformer. Compared with the baseline only using sparse convolution module, adding the transformer layer improves all metrics on FlyingThings3D, as reported in the third row in Table 2. This indicates that the transformer can pro-

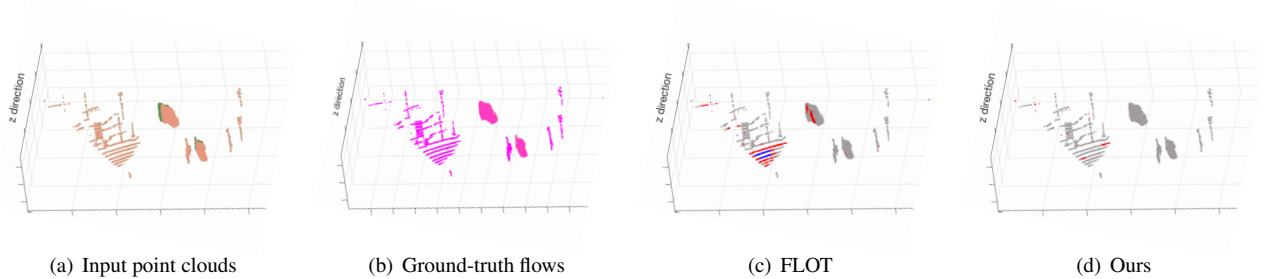


Figure 5: **Qualitative comparisons between FLOT [39] and our method.** Orange and green indicates the first and second point clouds in (a). The similar color indicates the point cloud has the similar flows in (b). Gray, red and blue color indicate small, medium and large errors in (c)(d).

vide important information for scene flow. As for KITTI, Table 2 shows that adding the transformer module significantly improve the flow estimation accuracy. For example, EPE3D is improved by 11.1%, compared with only using the sparse convolution module. This indicates that the transformer module improves the generalization capability of our method, since it provides complementary improvement to the sparse convolution module. For example, since our sparse convolution module suffers the issue of information loss, only using this module inevitably leads to inaccurate flow prediction for regions with large information loss. However, our transformer module explicitly learns point relations, which provides rich contextual information and helps to match corresponding points even for objects with complex structures.

FSC loss. Table 2 shows that adding the FSC loss helps achieving better scene flow estimation on KITTI. Yet, it display only minor improvement on FlyingThings3D, mostly on the metrics Acc3DS, Acc3DR and Outliers. Our FSC loss further helps improving the generalization capability of our method.

4.4. Ablation over FLOT

We incorporate our proposed transformer module and FSC loss with a recent state-of-the-art method FLOT [39] in order to evaluate further the effectiveness of these two modules. As shown in Table 3, both our proposed transformer module and FSC loss improves the flow prediction accuracy by a significant margin. In particular, FLOT adopts PointNet++ [41] as their feature extraction, where PointNet++ aggregates feature for points from local regions without explicitly considering point relation. The results shows that such feature is still insufficient for scene flow estimation. In other words, our transformer module, which explicitly models points relation, significantly improving the performance of FLOT on both KITTI and Flythings3D, with an EPE3D reduced to 0.043.

The FCS loss on top of FLOT achieves comparable results with FLOT on Flythings3D, yet the performance on

Table 4: **Running time comparisons.** The runtime of FLOT [39], PointPWC [62] and our method SCTN are evaluated on a single GTX2080Ti GPU. We used the official implementation of FLOT and pointPWC.

Method	Runtime (ms)
PointPWC [62]	149.6
FLOT [39]	389.3
SCTN (ours)	202.7

KITTI are better, showing that the FSC loss improves the generalization capability of FLOT. Overall, our FSC loss and transformer are complementary and can improve the flow accuracy of other scene flow estimation methods.

4.5. Runtime

We evaluate the running time of our method. Table 4 reports the evaluated time compared with recent state-of-the-art methods. FLOT [39] is the most related work to our method, since we both adopt point-wise correlations to generate predicted flows. Our method consumes lower running time than FLOT, although the transformer module is equipped.

5. Conclusion

We present a Sparse Convolution-Transformer Network (SCTN) for scene flow estimation. Our SCTN leverages the sparse convolution module to transfer irregular point cloud into locally consistent flow features for estimating spatially coherent motions in local regions. Our transformer module learns rich contextual information via explicitly modeling point relations, which is helpful for matching corresponding points and benefits scene flow estimation. A novel FSC loss is also proposed for training SCTN, improving the generalization ability of our method. We test our approach on FlyingThings3D and KITTI Scene Flow datasets, displaying state-of-the-art performances.

References

- [1] Michael J Black and Padmanabhan Anandan. A framework for the robust estimation of optical flow. In *1993 (4th) International Conference on Computer Vision*, pages 231–236. IEEE, 1993.
- [2] Thomas Brox, Christoph Bregler, and Jitendra Malik. Large displacement optical flow. In *2009 IEEE Conference on Computer Vision and Pattern Recognition*, pages 41–48. IEEE, 2009.
- [3] Nicolas Carion, Francisco Massa, Gabriel Synnaeve, Nicolas Usunier, Alexander Kirillov, and Sergey Zagoruyko. End-to-end object detection with transformers. In *Proceedings of the European Conference on Computer Vision (ECCV)*, pages 213–229, 2020.
- [4] Angel X. Chang, Thomas Funkhouser, Leonidas Guibas, Pat Hanrahan, Qixing Huang, Zimo Li, Silvio Savarese, Manolis Savva, Shuran Song, Hao Su, Jianxiong Xiao, Li Yi, and Fisher Yu. ShapeNet: An information-rich 3D model repository. Technical Report arXiv:1512.03012 [cs.GR], arXiv preprint, 2015.
- [5] Xinlei Chen and Kaiming He. Exploring simple siamese representation learning, 2020.
- [6] Yuhua Chen, Luc Van Gool, Cordelia Schmid, and Cristian Sminchisescu. Consistency guided scene flow estimation. In *European Conference on Computer Vision*, pages 125–141. Springer, 2020.
- [7] Lenaic Chizat, Gabriel Peyré, Bernhard Schmitzer, and François-Xavier Vialard. Scaling algorithms for unbalanced optimal transport problems. *Mathematics of Computation*, 87(314):2563–2609, 2018.
- [8] Christopher Choy, JunYoung Gwak, and Silvio Savarese. 4d spatio-temporal convnets: Minkowski convolutional neural networks. In *Proceedings of the IEEE Conference on Computer Vision and Pattern Recognition*, pages 3075–3084, 2019.
- [9] Marco Cuturi. Sinkhorn distances: lightspeed computation of optimal transport. In *Advances in Neural Information Processing Systems (NIPS)*, volume 2, page 4, 2013.
- [10] Ayush Dewan, Tim Caselitz, Gian Diego Tipaldi, and Wolfram Burgard. Rigid scene flow for 3d lidar scans. In *2016 IEEE/RSJ International Conference on Intelligent Robots and Systems (IROS)*, pages 1765–1770. IEEE, 2016.
- [11] Alexey Dosovitskiy, Philipp Fischer, Eddy Ilg, Philip Hausser, Caner Hazirbas, Vladimir Golkov, Patrick Van Der Smagt, Daniel Cremers, and Thomas Brox. FlowNet: Learning optical flow with convolutional networks. In *Proceedings of the IEEE international conference on computer vision*, pages 2758–2766, 2015.
- [12] Nico Engel, Vasileios Belagiannis, and Klaus Dietmayer. Point transformer, 2020.
- [13] Andreas Geiger, Philip Lenz, Christoph Stiller, and Raquel Urtasun. Vision meets robotics: The kitti dataset. *The International Journal of Robotics Research*, 32(11):1231–1237, 2013.
- [14] Zan Gojcic, Or Litany, Andreas Wieser, Leonidas J Guibas, and Tolga Birdal. Weakly Supervised Learning of Rigid 3D Scene Flow, 2021.
- [15] Xiuye Gu, Yijie Wang, Chongruo Wu, Yong Jae Lee, and Panqu Wang. Hplflownet: Hierarchical permutohedral lattice flownet for scene flow estimation on large-scale point clouds. In *Proceedings of IEEE Conference on Computer Vision and Pattern Recognition (CVPR)*, 2019.
- [16] Meng-Hao Guo, Jun-Xiong Cai, Zheng-Ning Liu, Tai-Jiang Mu, Ralph R. Martin, and Shi-Min Hu. Pct: Point cloud transformer, 2021.
- [17] Berthold KP Horn and Brian G Schunck. Determining optical flow. *Artificial intelligence*, 17(1-3):185–203, 1981.
- [18] Frédéric Huguet and Frédéric Devernay. A variational method for scene flow estimation from stereo sequences. In *2007 IEEE 11th International Conference on Computer Vision*, pages 1–7. IEEE, 2007.
- [19] Tak-Wai Hui and Chen Change Loy. Liteflownet3: Resolving correspondence ambiguity for more accurate optical flow estimation. In *European Conference on Computer Vision*, pages 169–184. Springer, 2020.
- [20] Tak-Wai Hui, Xiaoou Tang, and Chen Change Loy. Liteflownet: A lightweight convolutional neural network for optical flow estimation. In *Proceedings of the IEEE conference on computer vision and pattern recognition*, pages 8981–8989, 2018.
- [21] Eddy Ilg, Nikolaus Mayer, Tomoy Saikia, Margret Keuper, Alexey Dosovitskiy, and Thomas Brox. FlowNet 2.0: Evolution of optical flow estimation with deep networks. In *Proceedings of the IEEE conference on computer vision and pattern recognition*, pages 2462–2470, 2017.
- [22] Eddy Ilg, Tomoy Saikia, Margret Keuper, and Thomas Brox. Occlusions, motion and depth boundaries with a generic network for disparity, optical flow or scene flow estimation. In *Proceedings of the European Conference on Computer Vision (ECCV)*, pages 614–630, 2018.
- [23] Hani Itani, Silvio Giancola, Ali Thabet, and Bernard Ghanem. Sala: Soft assignment local aggregation for 3d semantic segmentation. *arXiv preprint arXiv:2012.14929*, 2020.
- [24] Huaizu Jiang, Deqing Sun, Varun Jampani, Zhaoyang Lv, Erik Learned-Miller, and Jan Kautz. Sense: A shared encoder network for scene-flow estimation. In *Proceedings of the IEEE/CVF International Conference on Computer Vision*, pages 3195–3204, 2019.
- [25] Diederik P Kingma and Jimmy Ba. Adam: A method for stochastic optimization. *arXiv preprint arXiv:1412.6980*, 2014.
- [26] Yair Kittenplon, Yonina C. Eldar, and Dan Raviv. Flowstep3d: Model unrolling for self-supervised scene flow estimation, 2020.
- [27] Huan Lei, Naveed Akhtar, and Ajmal Mian. Spherical kernel for efficient graph convolution on 3d point clouds. *IEEE transactions on pattern analysis and machine intelligence*, 2020.
- [28] Yangyan Li, Rui Bu, Mingchao Sun, Wei Wu, Xinhan Di, and Baoquan Chen. Pointcnn: Convolution on χ -transformed points. In *Proceedings of the 32nd International Conference on Neural Information Processing Systems*, pages 828–838, 2018.

- [29] Xingyu Liu, Charles R Qi, and Leonidas J Guibas. FlowNet3d: Learning scene flow in 3d point clouds. In *Proceedings of IEEE Conference on Computer Vision and Pattern Recognition (CVPR)*, 2019.
- [30] Ze Liu, Han Hu, Yue Cao, Zheng Zhang, and Xin Tong. A closer look at local aggregation operators in point cloud analysis. In *European Conference on Computer Vision*, pages 326–342. Springer, 2020.
- [31] Zhijian Liu, Haotian Tang, Yujun Lin, and Song Han. Point-voxel cnn for efficient 3d deep learning. In *Advances in Neural Information Processing Systems*, 2019.
- [32] Wei-Chiu Ma, Shenlong Wang, Rui Hu, Yuwen Xiong, and Raquel Urtasun. Deep rigid instance scene flow. In *IEEE Conference on Computer Vision and Pattern Recognition (CVPR)*, 2019.
- [33] Nikolaus Mayer, Eddy Ilg, Philip Häusser, Philipp Fischer, Daniel Cremers, Alexey Dosovitskiy, and Thomas Brox. A large dataset to train convolutional networks for disparity, optical flow, and scene flow estimation. In *Proceedings of the IEEE conference on computer vision and pattern recognition*, pages 4040–4048, 2016.
- [34] Moritz Menze, Christian Heipke, and Andreas Geiger. Object scene flow. *ISPRS Journal of Photogrammetry and Remote Sensing (JPRS)*, 2018.
- [35] Himangi Mittal, Brian Okorn, and David Held. Just go with the flow: Self-supervised scene flow estimation. In *Proceedings of the IEEE/CVF Conference on Computer Vision and Pattern Recognition (CVPR)*, June 2020.
- [36] N.Mayer, E.Ilg, P.Häusser, P.Fischer, D.Cremers, A.Dosovitskiy, and T.Brox. A large dataset to train convolutional networks for disparity, optical flow, and scene flow estimation. In *IEEE International Conference on Computer Vision and Pattern Recognition (CVPR)*, 2016.
- [37] N.Mayer, E.Ilg, P.Häusser, P.Fischer, D.Cremers, A.Dosovitskiy, and T.Brox. A large dataset to train convolutional networks for disparity, optical flow, and scene flow estimation. In *IEEE International Conference on Computer Vision and Pattern Recognition (CVPR)*, 2016.
- [38] Adam Paszke, Sam Gross, Francisco Massa, Adam Lerer, James Bradbury, Gregory Chanan, Trevor Killeen, Zeming Lin, Natalia Gimelshein, Luca Antiga, et al. Pytorch: An imperative style, high-performance deep learning library. *arXiv preprint arXiv:1912.01703*, 2019.
- [39] Gilles Puy, Alexandre Boulch, and Renaud Marlet. FLOT: Scene Flow on Point Clouds Guided by Optimal Transport. In *Proceedings of the European Conference on Computer Vision (ECCV)*, 2020.
- [40] Charles R Qi, Hao Su, Kaichun Mo, and Leonidas J Guibas. Pointnet: Deep learning on point sets for 3d classification and segmentation. In *Proceedings of the IEEE/CVF Conference on Computer Vision and Pattern Recognition (CVPR)*, pages 652–660, 2017.
- [41] Charles R Qi, Li Yi, Hao Su, and Leonidas J Guibas. Pointnet++: Deep hierarchical feature learning on point sets in a metric space. In *Advances in Neural Information Processing Systems*, pages 5099–5108, 2017.
- [42] Haozhe Qi, Chen Feng, Zhiguo Cao, Feng Zhao, and Yang Xiao. P2b: Point-to-box network for 3d object tracking in point clouds. In *Proceedings of the IEEE/CVF Conference on Computer Vision and Pattern Recognition*, pages 6329–6338, 2020.
- [43] Julian Quiroga, Thomas Brox, Frédéric Devernay, and James Crowley. Dense semi-rigid scene flow estimation from rgbd images. In *European Conference on Computer Vision*, pages 567–582. Springer, 2014.
- [44] René Ranftl, Kristian Bredies, and Thomas Pock. Non-local total generalized variation for optical flow estimation. In *European Conference on Computer Vision*, pages 439–454. Springer, 2014.
- [45] Olaf Ronneberger, Philipp Fischer, and Thomas Brox. U-net: Convolutional networks for biomedical image segmentation. In *International Conference on Medical image computing and computer-assisted intervention*, pages 234–241. Springer, 2015.
- [46] Shaoshuai Shi, Chaoxu Guo, Li Jiang, Zhe Wang, Jianping Shi, Xiaogang Wang, and Hongsheng Li. Pv-rcnn: Point-voxel feature set abstraction for 3d object detection. In *Proceedings of the IEEE/CVF Conference on Computer Vision and Pattern Recognition*, pages 10529–10538, 2020.
- [47] Deqing Sun, Erik B Sudderth, and Hanspeter Pfister. Layered rgbd scene flow estimation. In *Proceedings of the IEEE Conference on Computer Vision and Pattern Recognition*, pages 548–556, 2015.
- [48] Deqing Sun, Xiaodong Yang, Ming-Yu Liu, and Jan Kautz. Pwc-net: Cnns for optical flow using pyramid, warping, and cost volume. In *Proceedings of the IEEE/CVF Conference on Computer Vision and Pattern Recognition (CVPR)*, 2018.
- [49] Haotian* Tang, Zhijian* Liu, Shengyu Zhao, Yujun Lin, Ji Lin, Hanrui Wang, and Song Han. Searching efficient 3d architectures with sparse point-voxel convolution. In *Proceedings of the European Conference on Computer Vision (ECCV)*, 2020.
- [50] Zachary Teed and Jia Deng. Raft-3d: Scene flow using rigid-motion embeddings. *arXiv preprint arXiv:2012.00726*, 2020.
- [51] Zachary Teed and Jia Deng. Raft: Recurrent all-pairs field transforms for optical flow. In *European Conference on Computer Vision*, pages 402–419. Springer, 2020.
- [52] Hugues Thomas, Charles R Qi, Jean-Emmanuel Deschaud, Beatriz Marcotegui, François Goulette, and Leonidas J Guibas. Kpconv: Flexible and deformable convolution for point clouds. In *Proceedings of the IEEE/CVF International Conference on Computer Vision*, pages 6411–6420, 2019.
- [53] Ivan Tishchenko, Sandro Lombardi, Martin R Oswald, and Marc Pollefeys. Self-supervised learning of non-rigid residual flow and ego-motion. *arXiv preprint arXiv:2009.10467*, 2020.
- [54] Arash K Ushani, Ryan W Wolcott, Jeffrey M Walls, and Ryan M Eustice. A learning approach for real-time temporal scene flow estimation from lidar data. In *2017 IEEE International Conference on Robotics and Automation (ICRA)*, pages 5666–5673. IEEE, 2017.
- [55] Sundar Vedula, Simon Baker, Peter Rander, Robert Collins, and Takeo Kanade. Three-dimensional scene flow. In *Proceedings of the Seventh IEEE International Conference on*

- Computer Vision (ICCV)*, volume 2, pages 722–729. IEEE, 1999.
- [56] Christoph Vogel, Konrad Schindler, and Stefan Roth. Piecewise rigid scene flow. In *Proceedings of the IEEE International Conference on Computer Vision*, pages 1377–1384, 2013.
- [57] Peng-Shuai Wang, Yang Liu, Yu-Xiao Guo, Chun-Yu Sun, and Xin Tong. *ACM Trans. Graph.*, 36(4):72:1–72:11, 2017.
- [58] Zirui Wang, Shuda Li, Henry Howard-Jenkins, Victor Prisacariu, and Min Chen. FlowNet3d++: Geometric losses for deep scene flow estimation. In *Proceedings of the IEEE/CVF Winter Conference on Applications of Computer Vision (WACV)*, March 2020.
- [59] Andreas Wedel, Clemens Rabe, Tobi Vaudrey, Thomas Brox, Uwe Franke, and Daniel Cremers. Efficient dense scene flow from sparse or dense stereo data. In *European conference on computer vision*, pages 739–751. Springer, 2008.
- [60] Philippe Weinzaepfel, Jerome Revaud, Zaid Harchaoui, and Cordelia Schmid. Deepflow: Large displacement optical flow with deep matching. In *Proceedings of the IEEE international conference on computer vision*, pages 1385–1392, 2013.
- [61] Wenxuan Wu, Zhongang Qi, and Li Fuxin. Pointconv: Deep convolutional networks on 3d point clouds. In *Proceedings of the IEEE/CVF Conference on Computer Vision and Pattern Recognition*, pages 9621–9630, 2019.
- [62] Wenxuan Wu, Zhi Yuan Wang, Zhuwen Li, Wei Liu, and Li Fuxin. Pointpwc-net: Cost volume on point clouds for (self-) supervised scene flow estimation. In *Proceedings of the European Conference on Computer Vision (ECCV)*, pages 88–107, 2020.
- [63] Zhirong Wu, Shuran Song, Aditya Khosla, Fisher Yu, Linguang Zhang, Xiaoou Tang, and Jianxiong Xiao. 3d shapenets: A deep representation for volumetric shapes. In *Proceedings of the IEEE conference on computer vision and pattern recognition*, pages 1912–1920, 2015.
- [64] Saining Xie, Jiatao Gu, Demi Guo, Charles R. Qi, Leonidas Guibas, and Or Litany. Pointcontrast: Unsupervised pre-training for 3d point cloud understanding. In *Proceedings of the European Conference on Computer Vision (ECCV)*, 2020.
- [65] Christopher Zach, Thomas Pock, and Horst Bischof. A duality based approach for realtime tv-l1 optical flow. In *Joint pattern recognition symposium*, pages 214–223. Springer, 2007.
- [66] Jesus Zarzar, Silvio Giancola, and Bernard Ghanem. Efficient tracking proposals using 2d-3d siamese networks on lidar. *arXiv preprint arXiv:1903.10168*, 2019.
- [67] Jesus Zarzar, Silvio Giancola, and Bernard Ghanem. Pointrgcn: Graph convolution networks for 3d vehicles detection refinement. *arXiv preprint arXiv:1911.12236*, 2019.
- [68] Zhiyuan Zhang, Binh-Son Hua, and Sai-Kit Yeung. Shellnet: Efficient point cloud convolutional neural networks using concentric shells statistics. In *Proceedings of the IEEE/CVF International Conference on Computer Vision (ICCV)*, October 2019.
- [69] Hengshuang Zhao, Jiaya Jia, and Vladlen Koltun. Exploring self-attention for image recognition. In *Proceedings of the IEEE/CVF Conference on Computer Vision and Pattern Recognition (CVPR)*, June 2020.
- [70] Hengshuang Zhao, Li Jiang, Jiaya Jia, Philip Torr, and Vladlen Koltun. Point transformer, 2020.
- [71] Xizhou Zhu, Weijie Su, Lewei Lu, Bin Li, Xiaogang Wang, and Jifeng Dai. Deformable detr: Deformable transformers for end-to-end object detection. *arXiv preprint arXiv:2010.04159*, 2020.

6. Appendix

6.1. Qualitative Results on FlyingThings3D

We provide qualitative results of our method on FlyingThings3D dataset.

Figure 6 shows three examples where point clouds are with large motions (see large position differences between orange and green point cloud in Figure 6a). FLOT introduces medium errors in large regions of objects especially in uniform regions. In contrast, our method better predicts flows, since our transformer captures rich context information for finding correspondences and FSC loss adaptively enforces flow consistency.

Figure 7 shows three examples where point clouds containing complex scene or objects with complex structure. Our method achieves better performance than FLOT. Our transformer can learn meaningful structure information via explicitly modeling point relation.

In addition, we warp the first point cloud \mathcal{P} using the predicted scene flow and visualize the warped point cloud, like FLOT [39] and PointPWC [62] did. If the warped point cloud using predicted flows is similar to that using ground-truth flows, the predicted flows are of high accurate. As shown in Figure 8, since our method predicts higher accurate flows than FLOT, the warped point cloud using our predicted flows is more similar to that using ground-truth flows.

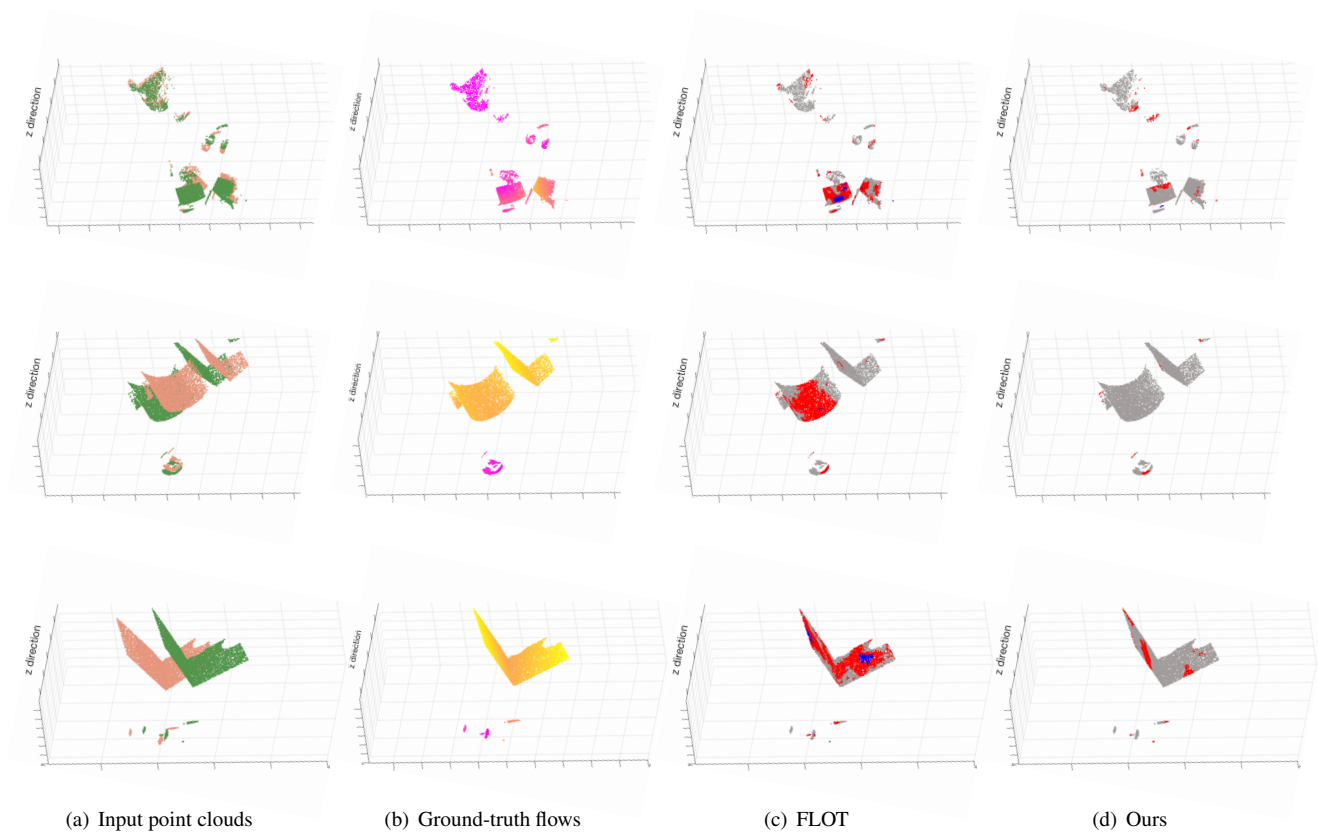


Figure 6: **Qualitative comparisons between FLOT [39] and our method on Flythings3D dataset.** Orange and green indicates the first and second point clouds in (a). The similar color indicates the point cloud has the similar flows in (b). Gray, red and blue color indicate small, medium and large errors in (c)(d).

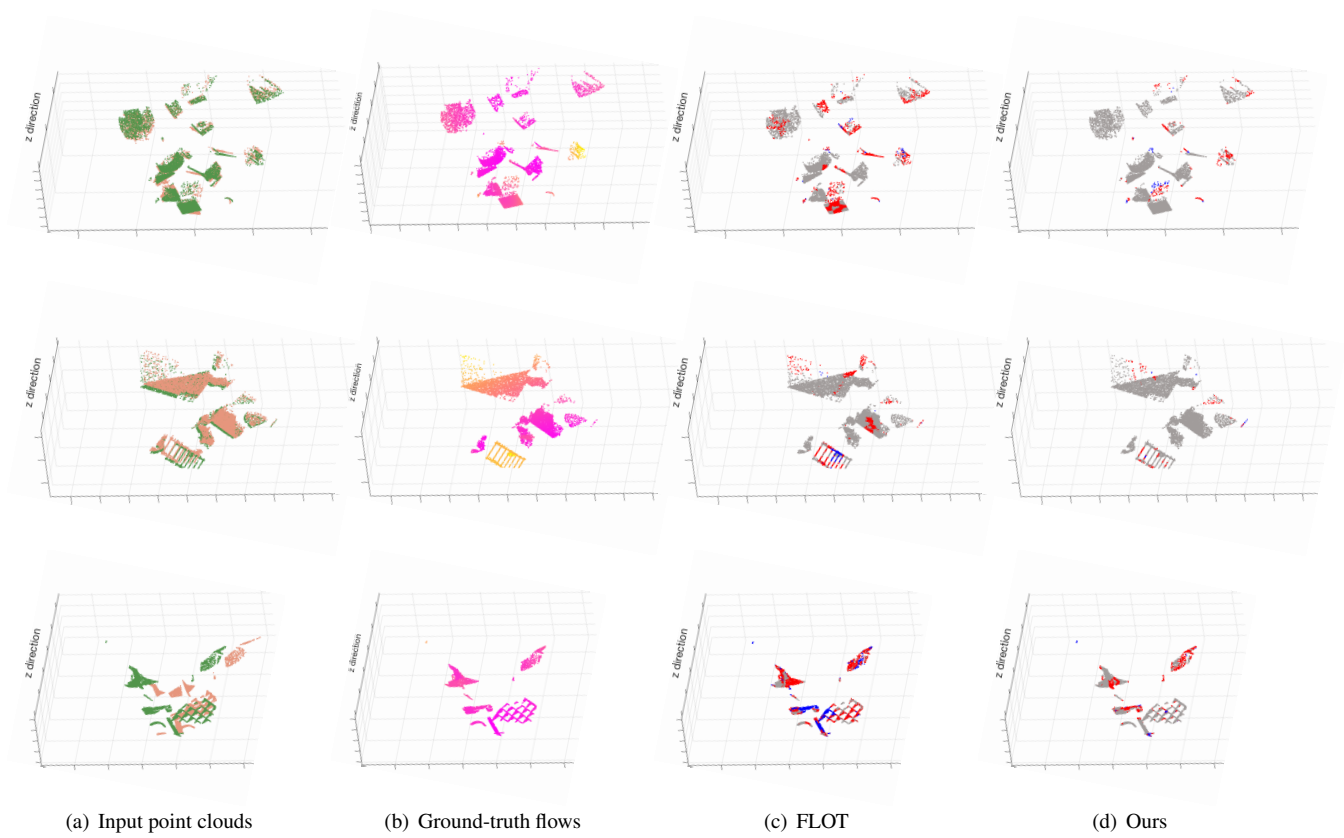


Figure 7: **Qualitative comparisons between FLOT [39] and our method on Flythings3D dataset.** Orange and green indicates the first and second point clouds in (a). The similar color indicates the point cloud has the similar flows in (b). Gray, red and blue color indicate small, medium and large errors in (c)(d).

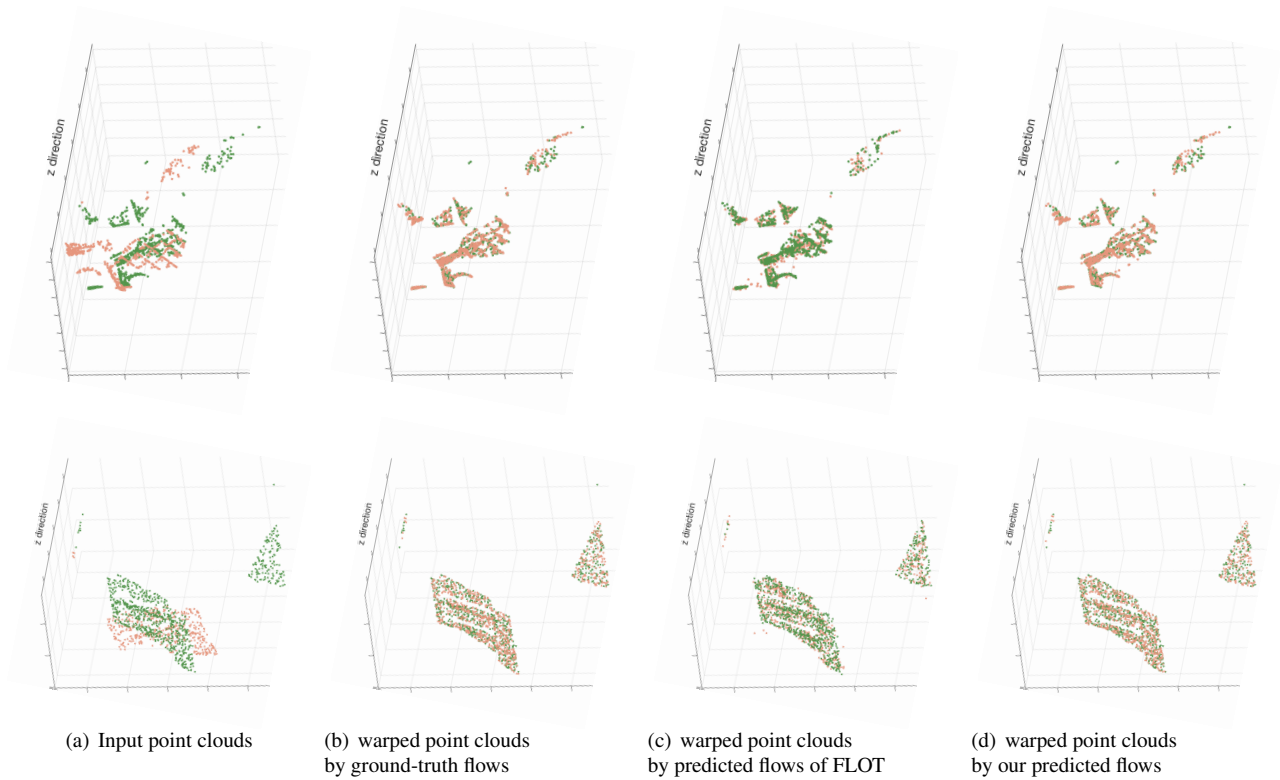


Figure 8: **Qualitative comparisons between FLOT [39] and our method on Flythings3D dataset.** Orange and green indicates the first and second point clouds in (a)(b)(c)(d). The first point cloud is warped by ground-truth flows in (b), and is warped by predicted flows of FLOT in (c) and our method in (d), respectively. Compared with FLOT, the warped first point cloud by our predicted flows is more similar to that by ground-truth flows, indicating better estimation accuracy of our method.